Scheme I

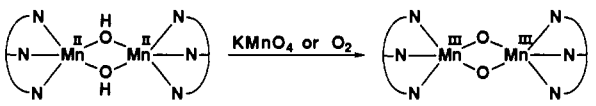

Å) is too short for the structure and there is some debate as to whether this might be a bis(μ-oxo)manganese(IV,IV) complex. The Mn–Mn separation of **2** (3.31 Å) is much longer than those reported for bis(μ-oxo) dinuclear manganese complexes (ca. 2.7 Å), and it is of interest that the value is close to a Mn–Mn separation known for PSII OEC. EXAFS studies on OEC showed two distinct Mn–Mn separations of 2.7 and 3.3 Å.[12] The shorter distance is associated with a bis(μ-oxo) moiety; however, the structural implications of the longer separation have not yet been unambiguously determined. The possibility of a μ-oxo bis(carboxylato) core structure was pointed out.[1c] On the basis of the XANES result, it is unlikely that the S_1 state of OEC contains two Mn(II) ions.[12] However, because the Mn–Mn separation primarily depends on the core structure rather than the oxidation state, the present result raises the new possibility that the 3.3-Å separation of OEC may be ascribed to a bis(μ-hydroxo) structure. The magnetic susceptibility of the powdered sample of **2** is 6.88 μ_B/mol at 298 K, indicative of a magnetically weak interaction between the two high-spin manganese(II) ions. This is further supported by the X-band EPR spectrum of **2** measured at 77 K, which showed very complicated features as known for magnetically weakly coupled dinuclear Mn(II,II) complexes.[13]

The anaerobic oxidation of **2** with $KMnO_4$ gave a bis(μ-oxo)manganese(III,III) complex (**3**) (Scheme I). In a typical experiment, the colorless solution of **2** was stirred with 4 equiv of $KMnO_4$ for 2 days in toluene. Unreacted $KMnO_4$ was removed by filtration, and the dark-red filtrate was evacuated to dryness under vacuum. Recrystallization of the resultant solid from pentane afforded **3**·C_5H_{12} as dark red crystals in ca. 90% yield.[14] The molecular structure of **3** is presented in Figure 2.[15] There is no crystallographically imposed center of symmetry. The Mn–O distances are in the range 1.79–1.81 Å, which are typical Mn–O bond distances for manganese–oxo bonds. The Mn–Mn separation of 2.70 Å is also typical for the dinuclear complexes having a Mn(μ-O)$_2$Mn moiety. There are many examples of bis(μ-oxo)-dimanganese complexes of Mn(III,IV) and Mn(IV,IV), whereas Mn(III,III) complexes were not known until very recently.[16] All these complexes contain six-coordinate manganese ions. On the other hand, the manganese ions in **3** are five-coordinate. This is attributable to the large steric hindrance of the present ligand. Complex **3** is EPR silent and gives a reasonably sharp ^{1}H NMR spectrum at low temperature. These facts together with the low magnetic susceptibility (2.81 μ_B/mol) suggest a strong antiferromagnetic interaction between the two manganese(III) ions in **3** as observed for other bis(μ-oxo)manganese(III) complexes,[16] although the coordination geometry is not comparable.

Complex **2** is also oxidatively converted to **3** under a dioxygen atmosphere. However, the yield to **3** was not very high (the highest yield was ca. 50%), and we noticed that at least two other manganese complexes are formed. Isolation and characterization of these species as well as further oxidation of **3** in the hope of evolving dioxygen are proceeding in this laboratory.

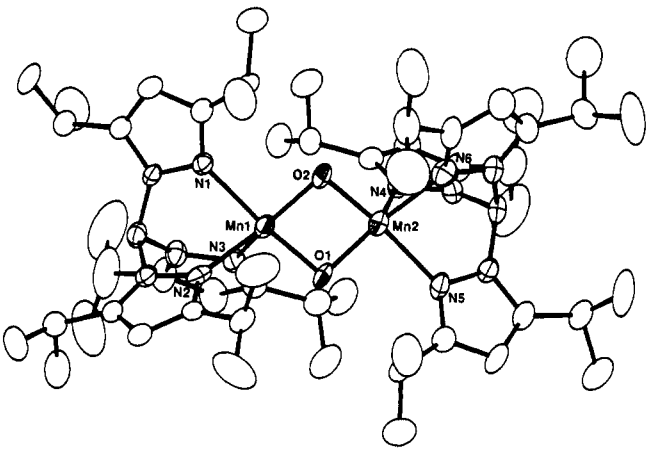

Figure 2. ORTEP view of [Mn(HB(3,5-iPr$_2$pz)$_3$)]$_2$(O)$_2$ (**3**). The solvent of crystallization is omitted for clarity. Selected bond distances (Å) and angles (deg): Mn1–O1, 1.806 (5); Mn1–O2, 1.813 (6); Mn1–N1, 2.084 (6); Mn1–N2, 2.099 (7); Mn1–N3, 2.228 (7); Mn2–O1, 1.808 (6); Mn2–O2, 1.787 (6); Mn2–N4, 2.224 (6); Mn2–N5, 2.093 (7); Mn2–N6, 2.084 (7); Mn1···Mn2, 2.696 (2); O1···O2, 2.369 (8); Mn1–O1–Mn2, 96.5 (3); Mn1–O2–Mn2, 97.0 (3).

Acknowledgment. This research was supported in part by a Grant-in-Aid for Scientific Research from the Ministry of Education, Science and Culture (02750589). We appreciate the kind editing of this manuscript by Professor L. Que, Jr., of University of Minnesota. The kind help in the X-ray analysis of **3**·C_5H_{12} by Dr. M. Tanaka in this institute is acknowledged.

Supplementary Material Available: Summary of X-ray analysis, atomic coordinates, anisotropic thermal parameters, and bond distances and angles for **2**·6CH_2Cl_2 and **3**·C_5H_{12} (24 pages); listing of observed and calculated structures factors for **2**·6CH_2Cl_2 and **3**·C_5H_{12} (45 pages). Ordering information is given on any current masthead page.

(12) (a) Graham, N. G.; Prince, R. C.; Cramer, S. P. *Science* **1989**, *243*, 789. (b) Penner-Hahn, J. E.; Fronko, R. M.; Pecoraro, V. L.; Yocum, C. F.; Betts, S. D.; Bowlby, N. R. *J. Am. Chem. Soc.* **1990**, *112*, 2549.

(13) (a) Mabad, B.; Cassoux, P.; Tuchagues, J.-P.; Hendrickson, D. N. *Inorg. Chem.* **1986**, *25*, 1420. (b) Mathur, P.; Crowder, M.; Dismukes, G. C. *J. Am. Chem. Soc.* **1987**, *109*, 5227. (c) Kessissoglou, D. P.; Butler, W. M.; Pecorado, V. L. *Inorg. Chem.* **1987**, *26*, 495.

(14) Satisfactory elemental analysis was obtained for **3** dried under vacuum. Anal. Calcd for $C_{54}H_{92}N_{12}O_2B_2Mn_2$: C, 60.39; H, 8.57; N, 15.65. Found: C, 60.09; H, 8.74; N, 15.80. IR: ν(BH), 2535 cm^{-1}. UV-vis [λ_{max}, nm (ϵ, cm^{-1} M^{-1})] (toluene): 468 nm (315). ^{1}H NMR (toluene-d_8, −40 °C): 1.43 (br, 72 H, *Me*$_2$CH), 5.75 (s, 6 H, Me$_2$C*H*), 6.95 (s, 6 H, Me$_2$C*H*), 8.96 (s, 6 H, pz).

(15) **3**·C_5H_{12} ($C_{59}H_{104}N_{12}O_2B_2Mn_2$; FW 1145.05) crystallized in the monoclinic space group $C2/c$ with a = 48.325 (9) Å, b = 15.747 (6) Å, c = 18.596 (2) Å, β = 106.21 (3)°, V = 13 588 (2) Å^3, and Z = 8. D_{calcd} = 1.12; D_{measd} = 1.12 ± 0.01 g cm^{-3}. The current R and R_w factors are 8.83% and 10.53% for 5420 reflections ($5° < 2\theta < 45°$, $F_o \geq 3\sigma F_o$).

(16) (a) Goodson, P. A.; Hodgson, D. J. *Inorg. Chem.* **1989**, *28*, 3606. (b) Goodson, P. A.; Oki, A. R.; Glerup, J.; Hodgson, D. J. *J. Am. Chem. Soc.* **1990**, *112*, 6248.

Gold Cluster Laden Polydiacetylenes: Novel Materials for Nonlinear Optics

Allan W. Olsen and Zakya H. Kafafi*

Optical Sciences Division, Naval Research Laboratory Washington, D.C. 20375

Received May 20, 1991

Since the early work of Maxwell-Garnett,[1] there has been an interest in the optical properties of metal clusters embedded in a dielectric medium. Many recent studies have been reported on the dispersion of metal clusters in organic polymers.[2] We are interested in embedding metal clusters in a special class of organic polymers, namely, nonlinear optical (NLO) polymers. We describe here the synthesis and characterization of gold cluster laden polydiacetylenes. Separately, gold clusters[3] and polydiacetylenes[4]

(1) Maxwell-Garnett, J. C. *Philos. Trans. R. Soc. London* **1904**, *203*, 385; **1906**, *205*, 237.

(2) For example, see: (a) Klabunde, K. J.; Habdas, J.; Treviño, G. C. *Chem. Mater.* **1989**, *1*, 481. (b) Laurent, C.; Kay, E. *J. Appl. Phys.* **1989**, *65*, 1717. (c) Andrews, M. P.; Ozin, G. A. *Chem. Mater.* **1989**, *1*, 174. (d) Olsen, A. W.; Kafafi, Z. H. *Proc. Symp. on Clusters and Cluster-Assembled Materials*; Materials Research Society: Pittsburgh, 1991; Vol. 206, p 175.

are of interest because of their own inherent optical nonlinearities. Taken together, in the form of a metal cluster/polydiacetylene composite, these materials hold special promise as nonlinear optical materials.

Gold clusters were dispersed in poly(diphenylbutadiyne) (poly-DPBD) and poly{5,7-dodecadiyne-1,12-diol-*co*-bis[((*n*-butoxycarbonyl)methyl)urethane]} (poly-4-BCMU). Gold vapor was cocondensed with a large excess of a diacetylene monomer (method 1) or an organic solvent for the polydiacetylene of interest (method 2) on the walls of a metal reactor[5] maintained at 77 K. Method 1 was used for the preparation of Au_x/poly-DPBD whereas Au_x/poly-4-BCMU was obtained by adding poly-4-BCMU to a nonaqueous gold colloid.

When Au atoms were cocondensed with DPBD, a dark brown matrix was formed. The solid matrix and solutions derived from it have been characterized by IR and UV/vis spectroscopies, transmission electron microscopy (TEM), and elemental analysis. The matrix consisted of several components that could be separated by their solubilities. Unreacted DPBD was by far the largest component of the matrix. A large excess of DPBD was provided during the cocondensation to act as a diluent and reduce the number of encounters between reactive Au species thereby favoring the formation of small gold clusters. The matrix was dissolved in toluene and filtered to remove larger than colloidal particles of gold. Addition of hexanes to the toluene-soluble filtrate caused the precipitation of what was characterized to be a Au_x/poly-DPBD composite while the DPBD remained in solution.

On the basis of elemental analysis of three Au_x/poly-DPBD composites, a gold volume fraction between 13.6% and 16.7% was estimated. This result reflects a significant increase, about 2 orders of magnitude, in the metal volume fraction in Au_x/poly-DPBD over that of the original matrix and is due to the partitioning of the Au clusters with the poly-DPBD.

The measured IR spectrum of Au_x/poly-DPBD was similar to that of the proposed ladder structure of poly-DPBD, prepared by thermal polymerization of DPBD at 185 °C.[6] The most dramatic spectral change was the complete disappearance of the C≡C stretching band measured at 2154 cm^{-1} for monomeric DPBD. Of the two structural forms earlier suggested for poly-DPBD, a polyene structure (I) and a polyacene or ladder structure (II),[6] the ladder type was favored upon cocondensation with gold.

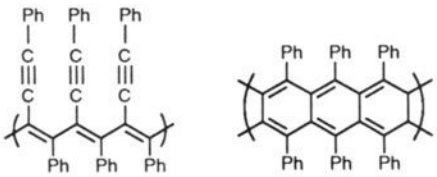

I II

TEM studies were carried out on the solid Au_x/DPBD/poly-DPBD matrix as it was prepared and on solutions derived from the matrix. Microscopy on the solid sample was performed to determine the size of the gold clusters prior to dissolution of the matrix. Figure 1a is a micrograph of the solid Au_x/DPBD/poly-DPBD matrix. An average cluster size of ~20 Å is estimated. Figure 1b is a micrograph of a Au_x/poly-DPBD composite obtained after exposure to toluene and hexane during the purification process and sample preparation for TEM measurements.

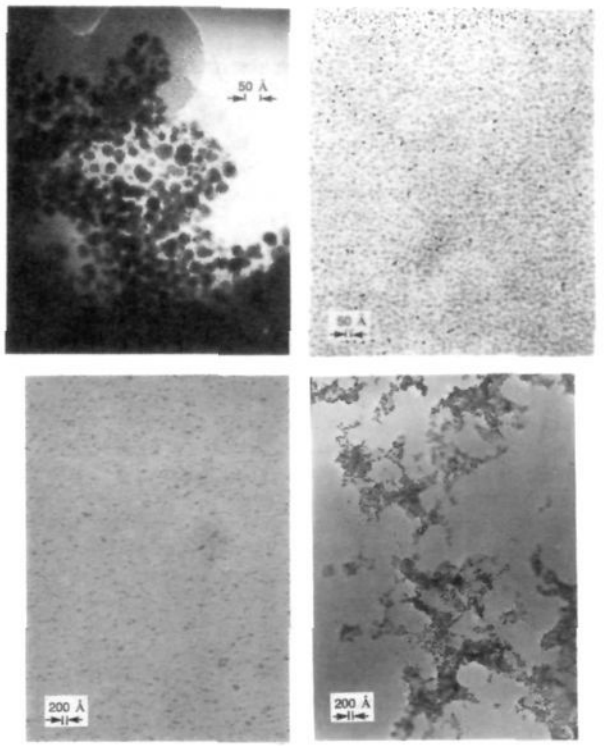

Figure 1. Transmission electron micrograms of (a) (upper left) solid Au_x/DPBD/poly-DPBD composite as prepared (magnification = 8×10^5); (b) (upper right) Au_x/poly-DPBD after purification (magnification = 2×10^5); (c) (lower left) Au_x/poly-4-BCMU (note the homogeneous dispersion) (magnification 5×10^4); and (d) (lower right) Au_x/acetone (note the extensive aggregation) (magnification = 5×10^4).

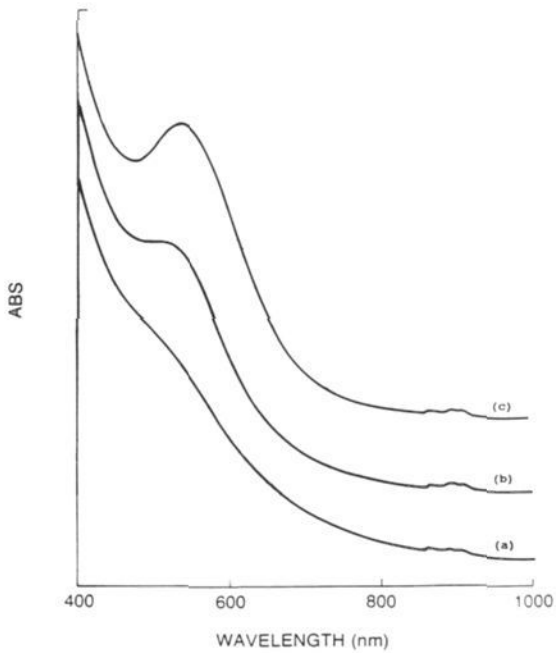

Figure 2. UV/vis spectra of an acetone solution of Au_x/DPBD/poly-DPBD (a) fresh, and aged for (b) 8 and (c) 35 days (note the growth of the cluster plasmon absorption as a function of time).

The average cluster size remained constant, ~20 Å. It is very common for metal clusters to aggregate into fractal-like structures when colloidal dispersions are dried on a TEM grid. One way to avoid such aggregation is to add a stabilizer (e.g., gelatin).[7] In this case it appears as though the poly-DPBD serves as the

(3) (a) Bloemer, M. J.; Haus, J. W.; Ashley, P. R. *J. Opt. Soc. Am. B* **1990**, *7*(5), 790. (b) Bloemer, M. J.; Ashley, P. R.; Haus, J. W.; Kalyaniwala, N.; Christensen, C. R. *J. Quant. Elect.* **1990**, *26*, 1075. (c) Dutton, T.; Van Wonterghem, B.; Saltiel, S.; Chestnoy, N. V.; Rentzepis, P. M.; Shen, T. R.; Rogovin, D. *J. Phys. Chem.* **1990**, *94*, 1100.

(4) (a) Messier, J. In *Nonlinear Optical Effects in Organic Polymers*; Messier, J., et al. Eds.; Kluwer Academic Publishers: Hingham, MA, 1989; p 47. (b) Sinclair, M.; McBranch, D.; Moses, D.; Heeger, A. J. *Appl. Phys. Lett.* **1988**, *3*, 2374. (c) Berkovic, G.; Superfine, R.; Guyot-Sionnest, P.; Shen, Y. R.; Prasad, P. N. *J. Opt. Soc. Am. B* **1988**, *5*, 668.

(5) (a) Klabunde, K. J.; Timms, P. L.; Skell, P. S.; Ittel, S. *Inorg. Synth.* **1979**, *19*, 59. (b) Lin, S. T.; Franklin, M. T.; Klabunde, K. J. *Langmuir* **1986**, *2*, 259.

(6) Berlin, A.; Cherkasin, M.; Chauser, M.; Shifrina, R. *Polym. Sci. USSR* **1967**, *9*(10), 2510.

(7) Kreibig, U. *Z. Phys. D: At., Mol. Clusters* **1986**, *3*, 239.

cluster stabilizer that prevents aggregation of the gold particles.

The presence of gold clusters in these polymeric composites was also evident from the metal plasmon absorption measured at ~530 nm. This plasmon absorption exhibited a noticeable solvent dependency as a function of time. When Au_x/DPBD/poly-DPBD dispersions were dissolved in either toluene or acetone, brown solutions were initially formed with identical UV/vis spectra. The toluene solution remained brown, and its spectrum did not change, whereas the acetone solution became reddish with time. The spectral changes, reflected in Figure 2, amount to the plasmon absorption band shifting to shorter wavelength and increasing in intensity. Several factors that influence plasmon absorptions are particle size and shape, the dielectric constant of the surrounding media, and the degree of aggregation of the metal particles.[7-9] A TEM study conducted on the same sample revealed that when a Au_x/DPBD/poly-DPBD matrix was dissolved in acetone, the gold clusters aggregated into fractal-like structures. Hence the protective polymeric layer that surrounds the metal cluster was attacked by acetone, leading to metal aggregation and change of the environment surrounding the cluster.

Gold clusters were dispersed in the well-characterized NLO polymer, poly-4-BCMU.[4] Poly-4-BCMU was also found to be very effective at preventing gold clusters from aggregating in solution. This result is indicated in the TEM shown in Figure 1c of Au_x/acetone to which a solution of poly-4-BCMU was added. Figure 1d shows the TEM of Au_x/acetone without poly-4-BCMU. The concentration of Au, relative to poly-4-BCMU, was increased by adding several Au_x/acetone colloids to a solution of poly-4-BCMU until the Au:poly-4-BCMU ratio was 1:1 by weight. Poly-4-BCMU is not readily soluble in acetone; therefore, large volumes of THF were used to ensure that the poly-4-BCMU remained in solution as each successive Au_x/acetone colloid was added. The final solution, although concentrated with respect to the Au:poly-4-BCMU ratio, was still too dilute for the nonlinear optical measurements. Concentration by simple evaporation of the solvent led to the formation of insoluble films on the sides of the glassware. Concentration by distilling away the solvent prevented the formation of films, but the effects of heating on the gold clusters are not known and are still under investigation. Notably, the colloid did not flocculate under reflux conditions. The 1:1 by weight Au_x/poly-4-BCMU solution was successfully concentrated by precipitating the Au_x/poly-4-BCMU composite with methanol and then dissolving it in a minimum amount of THF.

High-optical-quality films of Au_x/poly-4-BCMU were prepared by spin-coating but proved to be too thin (~1 μm) for the NLO measurements at 1.064 μm. The third-order NLO coefficient of solutions of Au_x/poly-4-BCMU was measured by degenerate four-wave mixing (DFWM) at 1.064 μm. For a composite with an estimated gold volume fraction of 7%, a 200-fold enhancement over that of pure poly-4-BCMU[4] was observed. The results of the study of the nonlinear optical properties of these composite materials will be discussed in detail in a future publication.

In summary, we have synthesized and characterized a new composite material, namely, metal cluster laden polydiacetylenes with potential nonlinear optical properties. Gold clusters have been embedded in poly-DPBD and poly-4-BCMU by metal vapor deposition. A large metal volume fraction of ~15% in poly-DPBD was achieved with an average cluster size of 20 Å. Preliminary NLO measurements on Au_x/poly-4-BCMU (metal volume fraction of 7%) indicated a 200-fold enhancement in the third-order optical coefficient of the composite material relative to that of the metal-free poly-4-BCMU.

Acknowledgment. We thank Dr. A. Snow for providing the poly-4-BCMU sample used in this study and Drs. F. Bartoli and R. Lindle for the DFWM measurements conducted on solutions of the composite materials. We also appreciate Dr. R. Pong's valuable contributions to this project. For financial support we acknowledge ONR, ONT, and DARPA.

(8) Kreibig, U.; Genzel, L. *Surf. Sci.* **1985**, *156*, 678.
(9) Papavassiliou, G. C. *Prog. Solid State Chem.* **1979**, *12*, 185.

Competing Redox and Inactivation Processes in the Inhibition of Cysteine Proteinases by Peptidyl *O*-Acylhydroxamates. ^{13}C and ^{15}N NMR Evidence for a Novel Sulfenamide Enzyme Adduct[1]

Valerie J. Robinson, Peter J. Coles, Roger A. Smith,* and Allen Krantz*

Syntex Research (Canada)
2100 Syntex Court, Mississauga, Ontario, Canada L5N 3X4

Received May 23, 1991

We recently reported the rapid inactivation of the cysteine proteinase cathepsin B by peptidyl *O*-acylhydroxamates (e.g., for **1**, inactivation rate k/K = 580000 M^{-1} s^{-1}).[2] This class of compounds was first described by Fischer and co-workers as irreversible inhibitors of serine proteinases such as α-chymotrypsin and dipeptidyl peptidase IV[3] and, more recently, as inhibitors of cysteine proteinases.[4] In this report, we describe ^{13}C and ^{15}N NMR characterization of the papain adduct obtained from the *O*-acylhydroxamate **1** as having a novel sulfenamide structure; as well, we have uncovered a rapid competing inhibition process that is normally masked by the presence of thiol reducing agent.

In our report of cathepsin B inactivation,[2] we proposed that the putative tetrahedral intermediate (**2**) could break down to give turnover products or could produce a stable adduct either by (a) migration of the peptidyl group in a manner similar to a Lossen (or related) rearrangement[5] to give a thiolcarbamate (e.g., **3**) or by (b) migration of the enzyme thiol group to afford a sulfenamide (e.g., **4**) (see Scheme I). To characterize the enzyme–inhibitor adduct and help clarify the mechanism of inactivation, ^{13}C- and ^{15}N-labeled *N*-(benzyloxycarbonyl)-L-phenylalanylglycine *O*-mesitoylhydroxamates (**1a**, labeled as $NHCH_2{}^{13}CONH$; **1b**, labeled as $NH{}^{13}CH_2{}^{13}CONH$; and **1c**, labeled as $NHCH_2{}^{13}CO{}^{15}NH$) were synthesized for NMR studies with papain.[6]

As in the case of cathepsin B in the presence of reducing thiol,[2] inactivation of papain was accompanied by some enzyme-catalyzed turnover of inhibitor, so that ca. 12 molar equiv of **1** was required for complete inactivation of the enzyme (pH 7, 5 mM 2-mercaptoethanol, 10 mM potassium phosphate). However, *in the absence of thiol*, papain activity could be completely inhibited with as little as a single molar equivalent of **1**. Inhibition of papain by **1c** in the absence of thiol, followed by removal of small molecules (MW <10000; Sepharose chromatography), provided a sample of inactive papain for which no ^{15}N or ^{13}C label could be detected by NMR measurement. The "small-molecule" fraction from this experiment consisted of $^{15}NH_4{}^+$ (by ^{15}N NMR: −360 ppm relative to nitromethane at 0 ppm), Z-Phe-$NHCH_2{}^{13}COOH$ (by HPLC and ^{13}C NMR: 179 ppm), and mesitoic acid (by HPLC). These byproducts represent an overall hydrolysis and reduction of **1c** by papain. Consistent with this observation, the inactive papain produced behaved as an oxidized enzyme, in that activity could be recovered (up to ca. 80%) by treatment with reducing thiol (e.g., 5 mM 2-mercaptoethanol). As well, treatment

(1) Contribution No. 344 from the Institute of Bioorganic Chemistry, Syntex Research.
(2) Smith, R. A.; Coles, P. J.; Spencer, R. W.; Copp, L. J.; Jones, C. S.; Krantz, A. *Biochem. Biophys. Res. Commun.* **1988**, *155*, 1201-1206.
(3) (a) Fischer, G.; Demuth, H.-U.; Barth, A. *Pharmazie* **1983**, *38*, 249-250. (b) Demuth, H.-U.; Baumgrass, R.; Schaper, C.; Fischer, G.; Barth, A. *J. Enzyme Inhib.* **1988**, *2*, 129-142. (c) Demuth, H.-U.; Neumann, U.; Barth, A. *J. Enzyme Inhib.* **1989**, *2*, 239-248.
(4) Bromme, D.; Schierhorn, A.; Kirschke, H.; Weideranders, B.; Barth, A.; Fittkau, S.; Demuth, H.-U. *Biochem. J.* **1989**, *263*, 861-866.
(5) (a) March, J. *Advanced Organic Chemistry*, 3rd ed.; Wiley-Interscience: New York, 1985; pp 982-990. (b) Groutas, W. C.; Stanga, M. A.; Brubaker, M. J. *J. Am. Chem. Soc.* **1989**, *111*, 1931-1932. (c) The species **3** could also conceivably arise from a Lossen rearrangement (possibly enzyme induced) of enzyme-bound **1**, rather than via intermediate **2**.
(6) Papain serves as a good model for the closely homologous cathepsin B enzyme: Takio, K.; Towatari, T.; Katanuma, N.; Teller, D. C.; Titani, K. *Proc. Natl. Acad. Sci. U.S.A.* **1983**, *80*, 3666-3670.

0002-7863/91/1513-7760$02.50/0